Supporting Information

Electrochemically induced Ostwald Ripening in Au/TiO_2 Nanocomposite

Xiao Liu[1,2], Daniel G. Stroppa[3,4,†], Marc Heggen[3,4], Yuri Ermolenko[5], Andreas Offenhäusser[1,2], and Yulia Mourzina[*,1,2]

[1] Peter Grünberg Institut-8, Forschungszentrum Jülich GmbH, 52425 Jülich, Germany

[2] Jülich Aachen Research Alliance (JARA)-Fundamentals of Future Information Technology, 52425 Jülich, Germany

[3] Peter Grünberg Institut-5 and [4] Ernst Ruska-Center, Forschungszentrum Jülich GmbH, 52425 Jülich, Germany

[5] Institute of Chemistry, St. Petersburg State University, 199034 St. Petersburg, Russia

[†] Present address: INL - International Iberian Nanotechnology Laboratory, 4715-330 Braga, Portugal

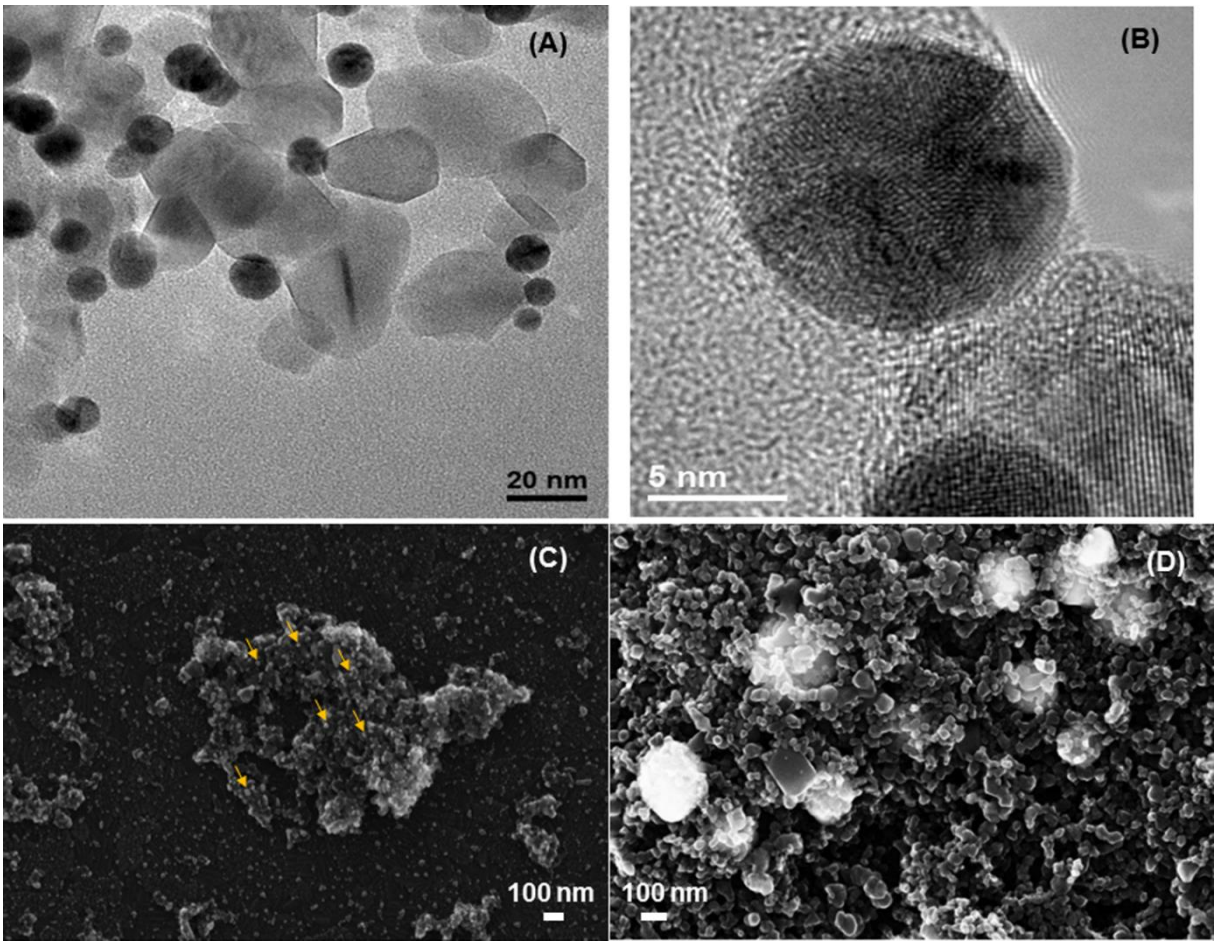

Figure S1. (A) TEM, (B) HRTEM and (C) SEM images of Au/TiO_2 nanocomposite before and (D) after 14 scans of electrochemical cycling in 0.1 M sulfuric acid; scan range 0 V to 1.5 V (Ag/AgCl, 3 M KCl); scan rate 0.05 Vs^{-1}. Arrows mark the Au NPs exemplarily.

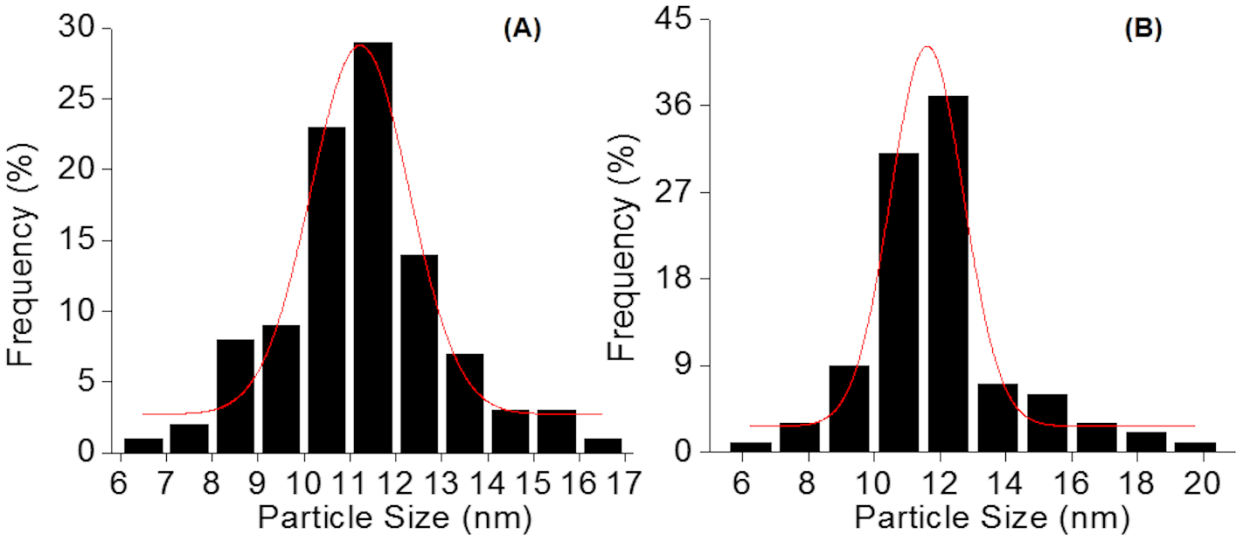

Figure S2. Histogram of the Au NPs distribution in: (A) Au/TiO_2 nanocomposite and (B) Au NPs.

Supporting information to section 3.2. It was also shown that the silver NPs on electrodes are more prone to oxidation than to reduction.[1] In the case of 12 nm gold NPs on the thin-film gold (bulk) electrodes (Figures S2 (B) and S5) without a nanoporous semiconductor matrix of TiO_2, we observed a negative (cathodic) shift of the reduction potential of the Au^+/Au^0 reaction during electrochemical redox cycling of about - 40 mV (Figure S7) compared to a thin-film gold electrode with a bulk value of the redox potential (~0.875 V against Ag/AgCl 3 M KCl), respectively. We assumed a symmetric shift of the oxidation (E_a) and reduction (E_c) potentials of the reaction $Au^+ + e \rightarrow Au^0$ and a reversible metal/metal ion redox potential $E' = (E_a + E_c)/2$.[2] The calculated shifts (eq. (3)) of the redox potential of about -0.033 V for the gold NPs of 12 nm diameter and of the peak oxidation potentials E_{pa} from 275 mV to 354 mV for the progressively increasing (diameter of 8–30 nm) citrate-stabilized Ag NPs attached to the ITO electrode via aminosilane[3] which were also calculated using eq. (3), corresponded well with the experimental values. However, in most cases, the effects were demonstrated for anodic stripping (oxidation potential) of silver NPs, which exhibited high reactivity and easy oxidation. The differences in electrochemical behavior in oxidation experiments using arrays of silver NPs on conductive surfaces were also studied for NPs with diameters greater than 25 nm under the assumption that these particles have the "bulk" value of the standard potential, E^0, of silver taking into account the size-dependent diffusion profile.[4]

Li et al. observed a negative (cathodic) shift of the reduction peak potential of a single Au NP electrode in comparison to the bulk value,[5] which the authors supposed was also due to the size effect. Cathodic potentials were shown to shift in the electrochemical deposition of gold NPs.[6-8] The effect observed here in the first scan is probably due to electrodeposition on different surfaces. During subsequent growth, which occurred on the gold sites, a further shift of the reduction potential to positive (bulk) values was observed. This could be due to increasing particle sizes, as discussed above.

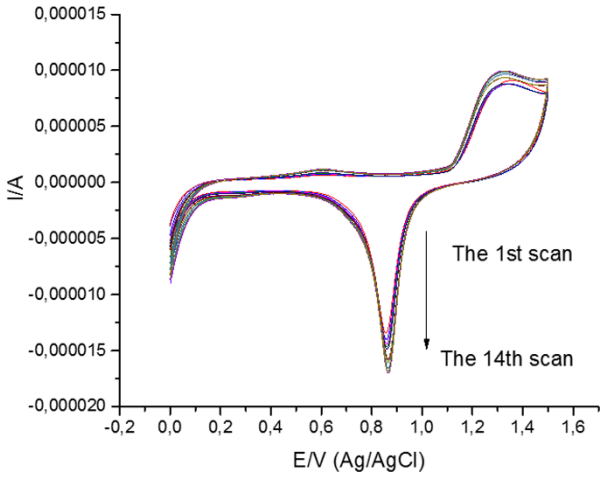

Figure S3. Cyclic voltammogramms of ITO/TiO_2-Au in 0.1 M sulfuric acid; scan range 0 V to 1.5 V (Ag/AgCl 3 M KCl); scan rate 0.05 Vs^{-1}.

Further studies may be required to explain some features of the voltamogramms of the nanocomposites. In particular, peak broadening and the distribution of redox potential values might be influenced by different weights of the exposed plane gold surfaces, defects and edges of the nanostructures, some dispersion in the nanoparticle size distribution, different potential drops in a nanoporous semiconductor matrix. Further factors, which may influence the voltammograms, are interaction of the electrical double layers of the nanoparticles, catalytic activity of the nanoparticles in the anodic region, local pH changes, microelectrode-type behavior, and electrical effects, such as the formation of the Schottky barrier at the TiO_2/Au boundary. Some of these effects should be also taken into the account in the case of Figure S6 and S7.

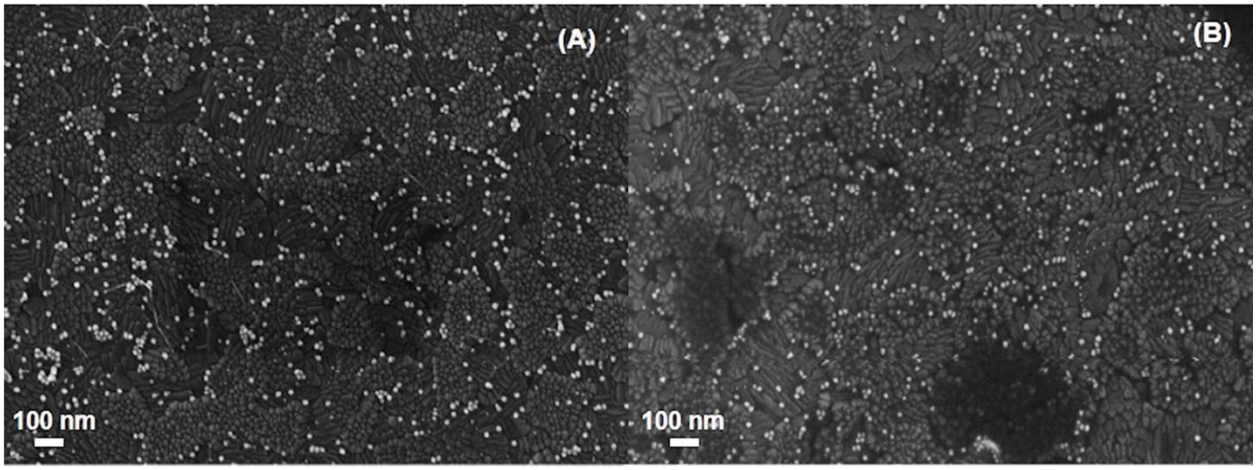

Figure S4. SEM images of ITO electrode modified with Au NPs (A) before and (B) after electrochemical cycling in 0.1 M sulfuric acid; scan range 0 V to 1.5 V (Ag/AgCl 3 M KCl); scan rate 0.05 Vs^{-1}.

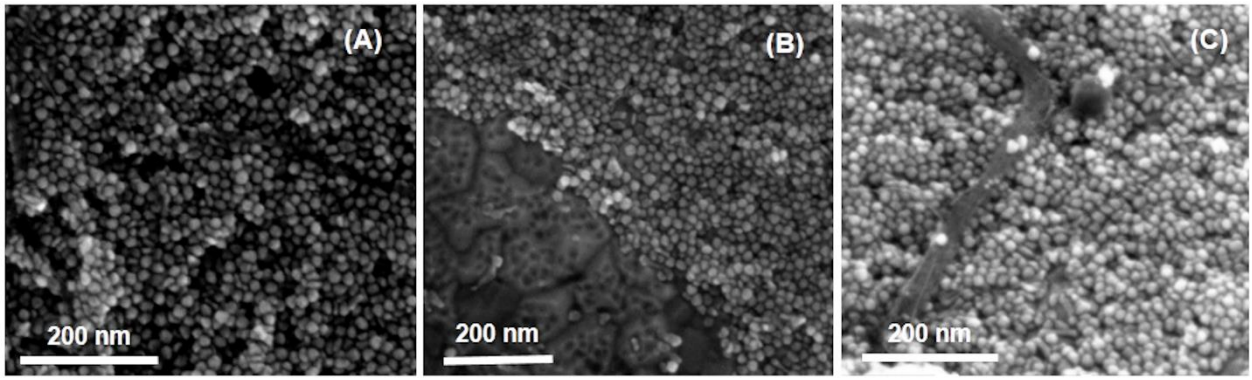

Figure S5. SEM images of thin-film gold electrode modified with Au NPs (A) before and (B) after electrochemical cycling in 0.1 M sulfuric acid. The indentations on the thin-film surface are visible where the particles were detached from the surface during electrochemical cycling. Scan range 0 V to 1.5 V (Ag/AgCl 3 M KCl); scan rate 0.05 Vs^{-1}. (C) SEM image of the electrode area outside the electrochemical cell.

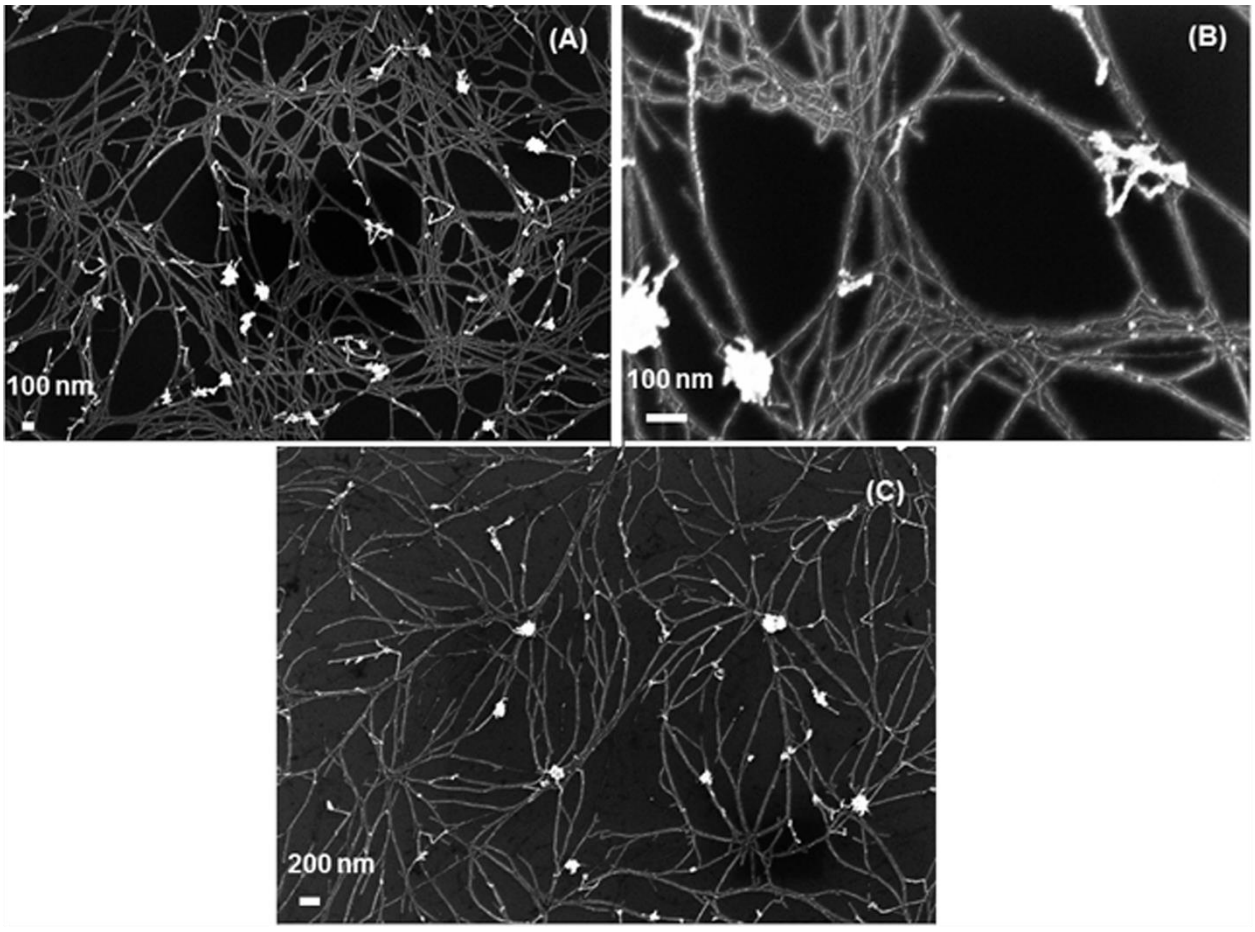

Figure S6. SEM images of Si/SiO_2 electrode modified with gold NWs (A,B) before and (C) after electrochemical cycling in 0.1 M sulfuric acid; scan range 0 V to 1.5 V (Ag/AgCl 3 M KCl); scan rate 0.05 Vs^{-1}.

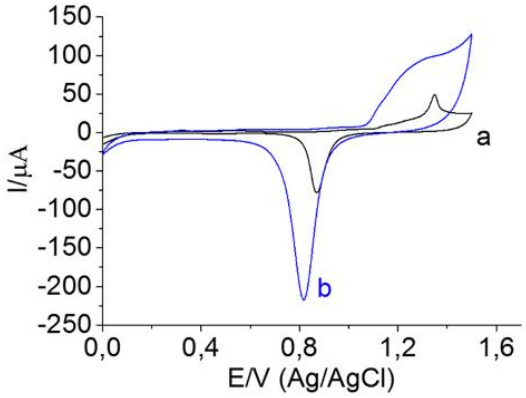

Figure S7. CVs of (a) bare thin-film gold electrode and (b) gold electrode modified with Au NPs in 0.1 M sulfuric acid; scan range 0 V to 1.5 V (Ag/AgCl 3 M KCl); scan rate 0.05 Vs^{-1}.

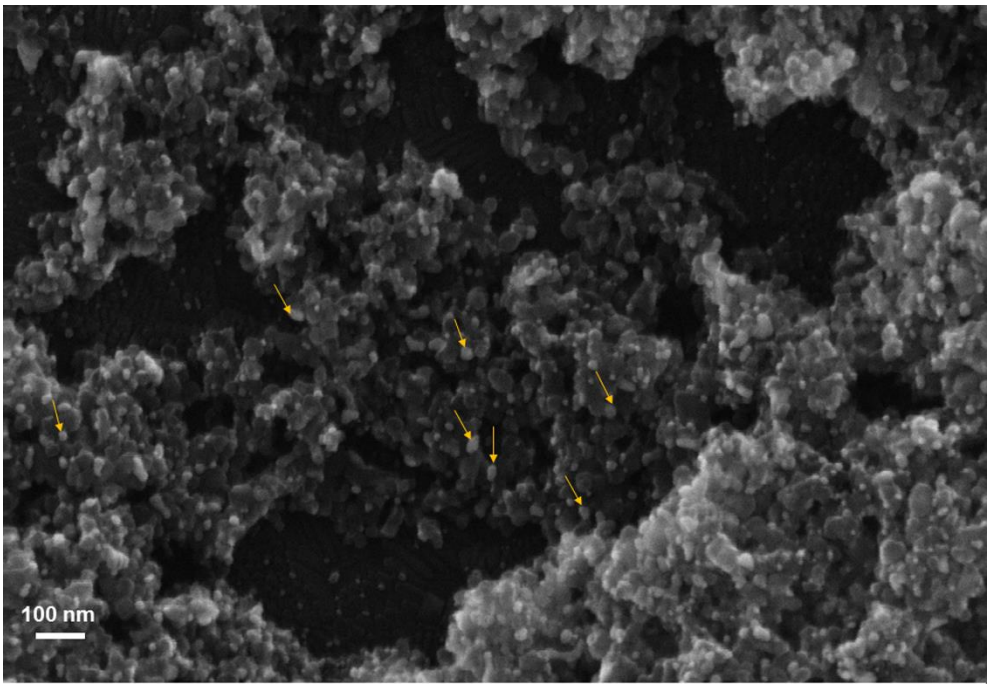

Figure S8. SEM image of the Au/TiO_2 nanocomposites on ITO after immersion in the growth solution for 9 weeks. Arrows mark the aggregated Au NPs.

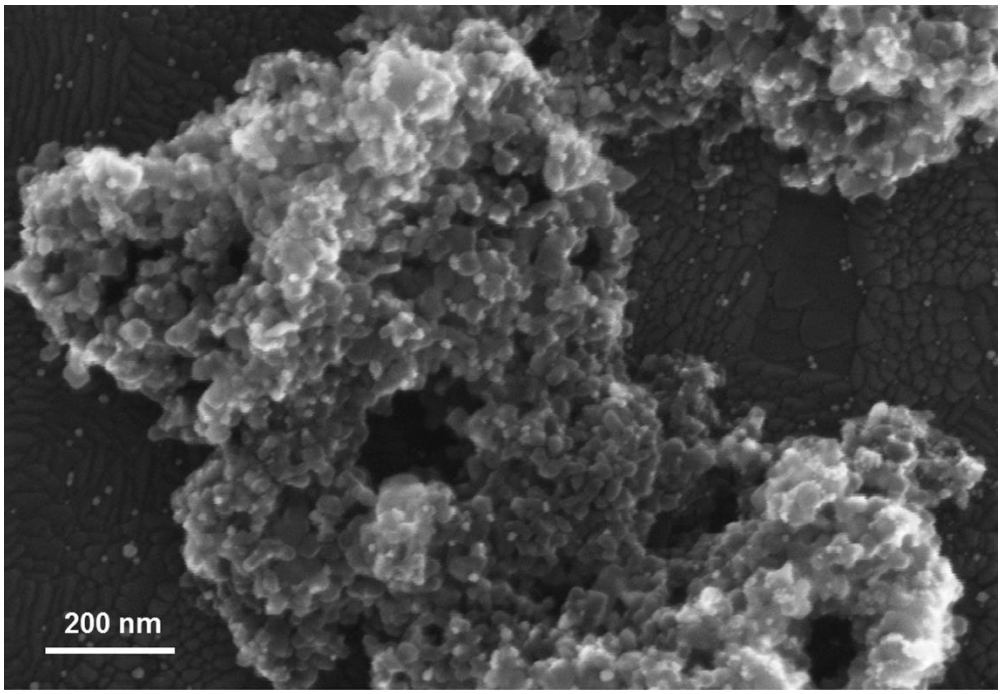

Figure S9. SEM image of Au/TiO_2 nanocomposites in 0.1 M sulfuric acid without applied potential under light for 4 days.

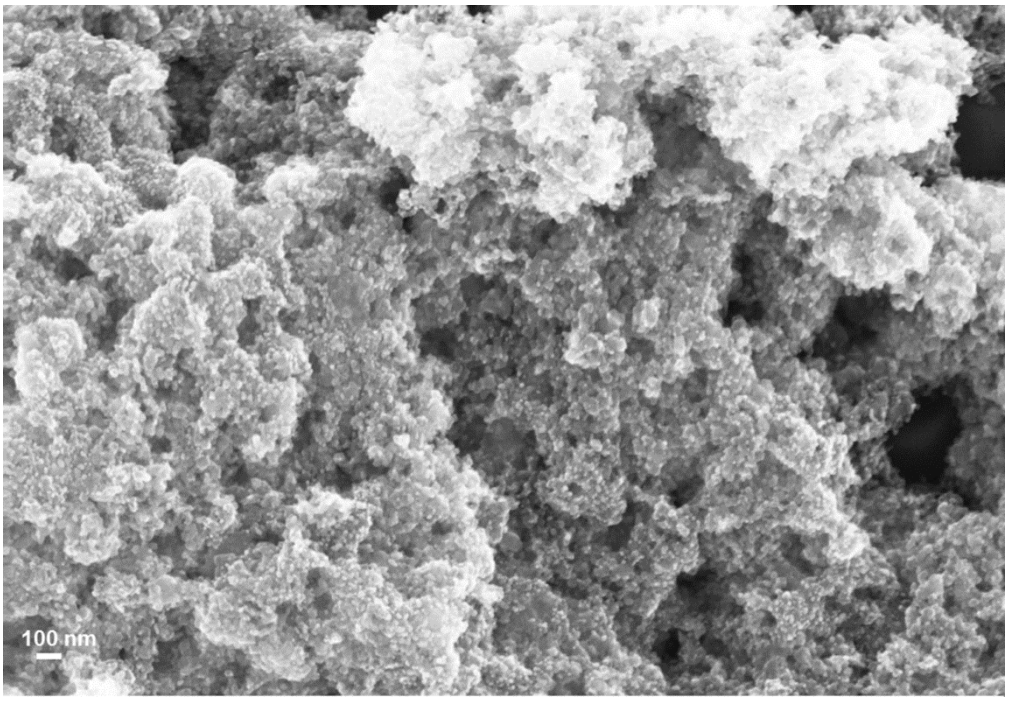

Figure S10 SEM image of Au/TiO_2 nanocomposites in 0.1 M sulfuric acid without applied potential and light for 4 days.

SI-Note (1) The concept of electrochemical potential of electron in the solution was developed by Reiss 1985,[9] Gerischer and Eckardt in 1983,[10] Bockris and Khan in 1987.[11] Although, there are no free electrons in the solutions as they are bound to ions, the application of this concept to electrochemical systems is accepted.

SI-Note (2) The electrochemical potential of electrons in a phase (1), $\tilde{\mu}_e^{(1)}$ is also referred to as Fermi energy (level) and corresponds to an electron energy $E_F^{(1)}$ representing an average energy of available electrons in phase (1), or more exactly, the energy where the occupation probability is 0.5 in the Fermi-Dirac distribution of electrons among the energy levels.[12]

SI-Note (3) Under the assumption that the mass and the surface charge density are kept constant during the dispersion process and neglecting the variation of γ (γ is the surface tension) on the potential, $(d\gamma/dE)_{T,p,N}=q_m$, Lippman equation for the excess charge on the interface q_m.[13]

References

(1) Chaki, N. K.; Sharma, J.; Mandle, A. B.; Mulla, I. S.; Pasricha, R.; Vijayamohanan, K. Size Dependent Redox Behavior of Monolayer Protected Silver Nanoparticles (2-7 nm) in Aqueous Medium. *Phys. Chem. Chem. Phys.* **2004**, *6*, 1304-1309.

(2) Bard, A. J.; Faulkner, L. R. *Electrochemical Methods: Fundamentals and Applications, 2nd Edition*; Wiley, New York, USA, 2001.

(3) Ivanova, O. S.; Zamborini, F. P. Size-Dependent Electrochemical Oxidation of Silver Nanoparticles. *J. Am. Chem. Soc.* **2009**, *132*, 70-72.

(4) Ward Jones, S. E.; Campbell, F. W.; Baron, R.; Xiao, L.; Compton, R. G. Particle Size and Surface Coverage Effects in the Stripping Voltammetry of Silver Nanoparticles: Theory and Experiment. *J. Phys. Chem. C* **2008**, *112*, 17820-17827.

(5) Li, Y.; Cox, J. T.; Zhang, B. Electrochemical Responses and Electrocatalysis at Single Au Nanoparticles. *J. Am. Chem. Soc.* **2010**, *132*, 3047-3054.

(6) Sheridan, E.; Hjelm, J.; Forster, R. J. Electrodeposition of Gold Nanoparticles on Fluorine-Doped Tin Oxide: Control of Particle Density and Size Distribution. *J. Electroanal. Chem.* **2007**, *608*, 1-7.

(7) Hezard, T.; Fajerwerg, K.; Evrard, D.; Collière, V.; Behra, P.; Gros, P. Gold Nanoparticles Electrodeposited on Glassy Carbon using Cyclic Voltammetry: Application to Hg (II) Trace Analysis. *J. Electroanal. Chem.* **2012**, *664*, 46-52.

(8) Wang, Y.; Laborda, E.; Ward, K. R.; Tschulik, K.; Compton, R. G. A Kinetic Study of Oxygen Reduction Reaction and Characterization on Electrodeposited Gold Nanoparticles of Diameter between 17 nm and 40 nm in 0.5 M Sulfuric Acid. *Nanoscale* **2013**, *5*, 9699-9708.

(9) Reiss, H. The Fermi Level and the Redox Potential. *J. Phys. Chem.* **1985**, *89*, 3783-3791.

(10) Gerischer, H.; Ekardt, W. Fermi Levels in Electrolytes and the Absolute Scale of Redox Potentials. *Appl. Phys. Lett.* **1983**, *43*, 393-395.

(11) Khan, S. U. M.; Kainthla, R. C.; Bockris, J. O. M. The Redox Potential and the Fermi Level in Solution. *J. Phys. Chem.* **1987**, *91*, 5974-5977.

(12) Hänsel, H.; Neumann, W. *Physik/Moleküle und Festkörper;* Spektrum Akademischer Verlag GmbH: Heidelberg, Berllin, Oxford, 1996.

(13) Frumkin, A. N.; Bagotsky, V. S.; Iofa, Z. A.; Kabanov, B. N. *Kinetics of Electrode Processes*; Moscow, 1952.